Article:
Rowland, L, Da Costa, ACL, Galbraith, DR et al. (2015) Death from drought in tropical forests is triggered by hydraulics not carbon starvation. Nature, 528 (7580). pp. 119-122. ISSN: 0028-0836

https://doi.org/10.1038/nature15539

Death from drought in tropical forests is triggered by hydraulics not carbon starvation

Rowland, L[1]., da Costa, A. C. L.[2], Galbraith, D. R[3]., Oliveira. R. S.[4], Binks, O. J.[1], Oliveira, A. A. R.[2], Pullen, A. M[5]., Doughty, C. E.[6], Metcalfe, D. B.[7], Vasconcelos, S. S.[8], Ferreira, L. V.[9], Malhi, Y.[6], Grace, J.[1], Mencuccini, M.[1,10] and Meir, P.[1,11]

[1] School of GeoSciences, University of Edinburgh, Edinburgh, UK

[2] Centro de Geosciências, Universidade Federal do Pará, Belém, Brasil

[3] School of Geography, University of Leeds, Leeds, UK

[4] Instituto de Biologia, UNICAMP, Campinas, Brasil

[5] The University of Cambridge, Cambridge, UK

[6] Environmental Change Institute, The University of Oxford, Oxford, UK

[7]Department of Physical Geography and Ecosystem Science, Lund University, Lund, Sweden

[8] EMBRAPA Amazônia Oriental, Belém, Brasil

[9] Museu Paraense Emílio Goeldi, Belém, Brasil

[10]ICREA at CREAF, 08193 Cerdanyola del Vallés, Spain

[11] Research School of Biology, Australian National University, Canberra, Australia

Drought threatens tropical rainforests over seasonal to decadal timescales[1-4], but the drivers of tree mortality following drought remain poorly understood[5,6]. It has been suggested that reduced availability of non-structural carbohydrates (NSC) critically increases mortality risk through insufficient carbon supply to metabolism ('carbon starvation')[7,8]. However little is known about how NSC stores are affected by drought, especially over the long term, and whether they are more important than hydraulic processes in determining drought-induced mortality. Using data from the world's longest-running experimental drought study in tropical

rainforest (in the Brazilian Amazon), we test whether carbon starvation or deterioration of the water-conducting pathways from soil to leaf trigger tree mortality. Biomass loss from mortality in the experimentally-droughted forest increased substantially after >10 years of reduced soil moisture availability. The mortality signal was dominated by the death of large trees, which were at a much greater risk of hydraulic deterioration than smaller trees. However, we find no evidence that the droughted trees suffered carbon starvation, as their NSC concentrations were similar to those of un-droughted trees, and growth rates did not decline in either living or dying individuals. Our results indicate that hydraulics, rather than carbon starvation, triggers tree death from drought in tropical rainforest.

Drought-response observations from both field-scale experiments and natural droughts have demonstrated increased mortality over the short-term (1-3 years), with notably higher vulnerability for some taxa, and for larger trees[6,9,10]. After several years of drought, recovering growth rates in smaller trees, dbh (diameter at breast height) <40 cm, and reduced mortality have been recorded at different locations[6,11,12]. However, the long-term (>10 yr) sensitivity of tropical forests to predicted prolonged and repeated water deficit[1-3] and the physiological mechanisms influencing this are poorly understood. Through-fall exclusion (TFE) studies, that create soil moisture deficit by the exclusion of a fraction of incoming rainfall, provide the only current means to assess the long-term response in mechanistic detail[5,13].

Trees experiencing drought stress are thought to die from direct physiological failure and/or from injury and biotic attack associated with a decline in physiological vigour[14]. A global effort to identify the relevant physiological mechanisms triggering death and thus to improve predictions of forest tree mortality has focussed on the twin possibilities of: (i) failure to

supply sufficient carbon substrate to metabolism following drought-related reductions in photosynthesis and increased use of NSC, theoretically leading to carbon starvation; and (ii) deterioration of the water-conducting xylem tissue, causing a rapid or gradual failure of key dependent processes (e.g., gas exchange, photosynthesis, phloem transport), and potentially leading to tissue desiccation[14,15], ultimately leading to mortality. Despite recent intensive research, it is unclear how important these two mechanisms are in different biomes and how, or whether, to model them[16].

Since 2002 a 50% TFE treatment has been implemented at a 1 ha-scale drought experiment in old-growth forest at Caxiuanã National Forest Reserve, Pará State, Brazil[6,12], to simulate possible rainfall reductions predicted to occur in parts of Amazonia by 2100[1]. Mortality surveys, recruitment and growth rates of all trees ≥10 cm dbh, have been monitored through the experimental period (see Methods). Recently, seasonal data on NSC concentrations were measured on leaves, branches and stems of 41 trees (20 trees on the control, 21 trees on the TFE) of the most common genera in the experiment (Extended Data Table 1). Xylem vulnerability curves were also performed on the branches of these trees (see Methods). Here, we synthesise these data to test whether long-term soil moisture deficit alters NSC storage and use in tropical rainforest trees, and if this, or hydraulic processes, are most strongly associated with increased mortality rates.

By 2014, following 13 years of the TFE treatment, cumulative biomass loss through mortality was 41.0±2.7% relative to pre-treatment values (Fig. 1a), and the rate of loss had increased substantially since the previous reported value of 17.2±0.8%, after 7 years of TFE[6]. Accelerating biomass loss and failure to recover substantially, or to reach a new equilibrium[13], has led to a committed flux to the atmosphere from decomposing necromass of 101.9±19.1 Mg C ha^{-1} (Fig. 1a). This biomass loss has been driven by elevated mortality in

the largest trees (Fig. 1b), as previously observed over shorter timescales[6], and has created a canopy that has had a persistently lower average leaf area index during 2010-2014 (12.0±1.2% lower; Extended data Fig. 1).

Remarkably, individual tree growth rates for the four years prior to death showed no significant reduction in either the TFE or control plots (Fig. 2a), indicating that growth is prioritised to the point of death irrespective of the soil moisture deficit treatment. From 2008, tree growth in every wet season (January-June) on the TFE treatment relative to the control was significantly elevated (P<0.05) in the small and medium trees (up to 4.6±0.2 times higher in small trees, and 2.9±0.2 times higher in medium trees), and maintained in the largest trees (10-20 cm, 20-40 cm and >40 cm dbh, respectively; Fig. 2b-d). Elevated wet season growth occurred despite 0.1-0.9 MPa reduction in average soil water potential (Ψ_s) at depths of 0-4 m on the TFE and a loss of seasonality in Ψ_s (Extended Data Fig. 2). Increased growth in the small trees occurred from 2008 onwards, following earlier substantial mortality of large trees (Fig. 1), which generated canopy gaps. Increased light availability to smaller trees, and presumably reduced below-ground competition for water and nutrients, allowed competitive release of trees on the TFE[8], and elevated growth rates. Competitive release on the TFE implies that, following 13 years of drought-stress, photosynthetic production is sufficient not only to maintain growth in the largest trees (Fig. 2d), but to increase growth in trees <40 cm dbh (Fig. 2b-c). This response would not be possible if the majority of trees were severely carbon limited, unless very considerable long-term (or renewed) carbon resources were being drawn upon.

Prioritisation of growth under drought in the TFE is consistent with recent observations following short-term drought in Amazonia[7]. However, the maintenance of NSC concentrations in the TFE treatment suggests that the prioritisation of growth during drought

97 does not occur at the expense of depleted carbon stores, as previously hypothesised[7]. Neither
98 the concentrations of soluble sugar (carbon immediately available to metabolism) nor starch
99 (stored carbon which can be converted to sugars) were significantly depleted in stem, leaf and
100 branch tissue from the TFE, relative to control (Fig. 3). The seasonal changes in both sugar
101 and starch concentrations, which varied by 50-90%, were much larger than any differences
102 associated with the TFE treatment (Fig. 3). Despite 13 years of severely reduced soil moisture
103 availability, the seasonal cycle and use of NSCs was unaltered, implying that the sampled
104 trees did not draw significantly upon their NSC reserves to buffer against the long-term
105 effects of soil moisture deficit. Large changes in carbon allocation from roots and leaves to
106 maintain stem growth during drought[17] have not been reported on the TFE[12]. Similarly no
107 drought-induced reductions in photosynthetic capacity occurred on the TFE[18], although how
108 total canopy productivity is affected remains uncertain. Considering this and additional
109 evidence of no increase in herbivore attack on the TFE (Extended Data Fig. 3), our results
110 suggest progressive carbon starvation and biotic foliar consumption are not important drivers
111 of the mortality patterns observed in the TFE forest following extended severe soil moisture
112 deficit (>10 years).

113 Deterioration of the water transport system in the xylem tissues following drought can also
114 lead to death[17,19]. The vulnerability of the xylem to drought is described by a vulnerability
115 curve[20], which relates water potential in xylem conduits to loss of hydraulic conductivity
116 because of occlusions by gas emboli. The water potential at which 50% loss of xylem
117 conductivity occurs ($P_{50,}$ MPa) is a commonly used index of embolism resistance[20]. We
118 determined xylem P_{50} for the trees on the control and TFE plots, with tree dbh ranging from
119 15 to 48 cm. A highly significant decrease in P_{50} with dbh was found across TFE and control
120 (Extended Data table 3, P<0.01). As dbh increased from 15 to 48 cm there was a 1.3±0.2
121 MPa reduction in the P_{50} value, with significant genus-to-genus differences (Fig.4). Leaf

water potential (Ψ_l) could only be measured during limited sampling campaigns (2-3 days) that were characterised by low vapour pressure deficit (VPD, 54-59% of peak dry season values) and unseasonal rainfall in the preceding days. Differences between treatment and control Ψ_l were not detected. Mean midday Ψ_l recorded across all the trees together with the vulnerability curves determined for each genus were used to predict the percentage loss of xylem conductivity (PLC) with dbh. Values of PLC at mean Ψ_l increased with dbh, with the largest diameter trees predicted to have reductions in conductive capacity of about 80% in some genera, indicating significant vulnerability to hydraulic deterioration (inset of Fig. 4).

Given no evidence of carbon starvation and similar Ψ_l across plots in the sample dates, why did many more trees die in TFE than control? The lack of treatment differences in Ψ_l contrasts starkly with the long-term records of lower Ψ_s (Extended Data Fig. 2). The lack of difference in midday Ψ_l could have been caused by sampling constraints or by isohydric behaviour. We found evidence of non-isohydric behaviour in our diurnal Ψ_l measurements (Extended Data Fig. 4), with overall strong linear declines in Ψ_l observed with increasing VPD on the control (R^2=0.18, P<0.01) and in particular on the TFE (R^2=0.33, P<0.01). Consequently limited sampling is the most likely cause of equal Ψ_l between the two plots, with TFE trees likely having more negative Ψ_l and lower hydraulic conductance during VPD maxima in the dry season. Reduced carbon uptake because of stomatal closure in some TFE trees is possible[21], but is unlikely to have caused carbon starvation considering growth rates were maintained or elevated on the TFE (Fig. 2) and radial growth should decline prior to photosynthesis in drought conditions[22]. Even with an isohydric response, trees on the TFE would still be likely to suffer greater hydraulic deterioration caused by greater PLC in the roots and main stem. Strongly reduced Ψ_s on the TFE (Extended Data Fig. 2) and significant hydraulic vulnerability of the tall trees are consistent with the hypothesis of hydraulic

deterioration as the most likely trigger of greater mortality, particularly in the largest trees, as observed. Why the xylem tissue of larger trees is more vulnerable to embolism deserves further study. Taller trees are predisposed to greater hydraulic stress, from elevated atmospheric demand and longer hydraulic path lengths[23]. As the canopies are exposed to rainfall in the TFE, smaller trees could avoid hydraulic deterioration through leaf water uptake[24-26], but this may not be sufficient to save the largest trees, which we hypothesise are forced to maintain their high growth rates until death to continually replace dysfunctional xylem.

Following decadal-scale soil moisture depletion, our results suggest tropical rainforests will experience accelerating biomass loss and a likely transition to a lower statured, lower biomass forest state, due to substantially elevated mortality of the largest trees. This mortality is most likely triggered by hydraulic processes, which lead to hydraulic deterioration and subsequent, potentially rapid, limitations in carbon uptake[21], instead of being caused directly by gradual carbon starvation. Under natural drought these forests may be under greater risk than from experimental drought, as severe soil moisture deficit is combined with low humidity and high air temperature increasing hydraulic demand. Improved prediction of the sensitivity of tropical tree mortality to drought should therefore focus on improved model simulation of plant hydraulics and modelling environmental controls on growth[27,22]. Decadal-scale ecological data such as these are rare, but they are invaluable for testing and improving predictions from vegetation models over timescales that are relevant to climate change[28]. They also underpin the long-term environmental policy needed to manage the natural capital that is embedded in tropical rainforests.

Author contributions

LR, PM, ALDC and MM designed and implemented the research. PM conceived and led the experiment and this study. LR led recent measurements; all authors contributed to data collection, led by ALDC. LR analysed the data with MM, PM, OB and AMP. LR wrote the paper with PM and MM, with contributions from all authors.

Acknowledgements:

This work is a product of UK NERC grant NE/J011002/1 to PM and MM, CNPQ grant 457914/2013-0/MCTI/CNPq/FNDCT/LBA/ESECAFLOR to ACLD, and ARC grant FT110100457 to PM. It was previously supported by NERC NER/A/S/2002/00487, NERC GR3/11706, EU FP5-Carbonsink and EU FP7-Amazalert to PM and JG, and by grant support to YM from NERC NE/D01025X/1 and the Gordon and Betty Moore Foundation. LR, MM and PM would also like to acknowledge support from Stephen Sitch, University of Exeter, Yann Salmon, University of Helsinki, Finland and Bradley Christoffersen, Los Alamos National Laboratory, USA. The authors would also like to thank three anonymous referees for their useful comments.

Author Information: Reprints and permissions information is available at www.nature.com/reprints. Correspondence and requests for materials should be addressed to lucy.rowland@ed.ac.uk.

References

1 Christensen, J. H. *et al.* in *Climate Change 2013: The Physical Science Basis. Contribution of Working Group I to the Fifth Assessment Report of the Intergovernmental Panel on Climate Change* (ed T.F. Stocker, Qin, D. , Plattner, G.-K., Tignor, M., Allen, S.K., Boschung, J., Nauels, A., Xia, Y., Bex, V., and Midgley, P.M. (eds.)) (Cambridge University Press, 2013).

2 Mora, C. *et al.* The projected timing of climate departure from recent variability. *Nature* 502, 183-187, doi:Doi 10.1038/Nature12540 (2013).

3 Reichstein, M. *et al.* Climate extremes and the carbon cycle. *Nature* 500, 287-295, doi:Doi 10.1038/Nature12350 (2013).

4 Boisier, J. P., Ciais, P., Ducharne, A. & Guimberteau, M. Projected strengthening of Amazonian dry season by constrained climate model simulations. *Nature Clim. Change* 5, 656-660, doi:10.1038/nclimate2658 (2015).

5 Hartmann, H., Adams, H. D., Anderegg, W. R. L., Jansen, S. and Zeppel, M. J. B. Research frontiers in drought-induced tree mortality: crossing scales and disciplines. *New Phytol*, 965-969, doi:doi: 10.1111/nph.13246 (2015).

6 da Costa, A. C. L. *et al.* Effect of 7 yr of experimental drought on vegetation dynamics and biomass storage of an eastern Amazonian rainforest. *New Phytol* 187, 579-591, doi:DOI 10.1111/j.1469-8137.2010.03309.x (2010).

7 Doughty, C. E. *et al.* Drought impact on forest carbon dynamics and fluxes in Amazonia. *Nature* 519, 78-U140, doi:Doi 10.1038/Nature14213 (2015).

8 O'Brien, M. J., Leuzinger, S., Philipson, C. D., Tay, J. & Hector, A. Drought survival of tropical tree seedlings enhanced by non-structural carbohydrate levels. *Nat Clim Change* 4, 710-714, doi:Doi 10.1038/Nclimate2281 (2014).

9 Nepstad, D. C., Tohver, I. M., Ray, D., Moutinho, P. & Cardinot, G. Mortality of large trees and lianas following experimental drought in an amazon forest. *Ecology* 88, 2259-2269, doi:Doi 10.1890/06-1046.1 (2007).

10 Phillips, O. L. *et al.* Drought Sensitivity of the Amazon Rainforest. *Science* 323, 1344-1347, doi:DOI 10.1126/science.1164033 (2009).

11 Brando, P. M. *et al.* Drought effects on litterfall, wood production and belowground carbon cycling in an Amazon forest: results of a throughfall reduction experiment. *Philos T R Soc B* 363, 1839-1848, doi:DOI 10.1098/rstb.2007.0031 (2008).

12 da Costa, A. C. L. *et al.* Ecosystem respiration and net primary productivity after 8-10 years of experimental through-fall reduction in an eastern Amazon forest. *Plant Ecol Divers* 7, 7-24, doi:Doi 10.1080/17550874.2013.798366 (2014).

13 Meir, P. *et al.* Threshold responses to soil moisture deficit by trees and soil in tropical rain forests: insights from field experiments. *Bioscience, in press* (2015).

14 McDowell, N. G. *et al.* The interdependence of mechanisms underlying climate-driven vegetation mortality. *Trends Ecol Evol* 26, 523-532, doi:DOI 10.1016/j.tree.2011.06.003 (2011).

15 Thomas, H. Senescence, ageing and death of the whole plant. *New Phytol* 197, 696-711, doi:Doi 10.1111/Nph.12047 (2013).

16 Meir, P., Mencuccini, M. & Dewar, R. C. Drought-related tree mortality: addressing the gaps in understanding and prediction. *New Phytol*, n/a-n/a, doi:10.1111/nph.13382 (2015).

17 Anderegg, W. R. L. *et al.* Drought's legacy: multiyear hydraulic deterioration underlies widespread aspen forest die-off and portends increased future risk. *Global Change Biol* 19, 1188-1196, doi:Doi 10.1111/Gcb.12100 (2013).

18 Rowland, L. *et al.* After more than a decade of soil moisture deficit, tropical rainforest trees maintain photosynthetic capacity, despite increased leaf respiration. *Global Change Biol* (2015), doi: Doi 10.1111/gcb.13035.

19 Anderegg, W. R. *et al.* The roles of hydraulic and carbon stress in a widespread climate-induced forest die-off. *Proc Natl Acad Sci U S A* 109, 233-237, doi:10.1073/pnas.1107891109 (2012).

20 Choat, B. *et al.* Global convergence in the vulnerability of forests to drought. *Nature* 491, 752-755, doi:10.1038/nature11688 (2012).

21 Sala, A., Woodruff, D. R. & Meinzer, F. C. Carbon dynamics in trees: feast or famine? Tree Physiol 32, 764-775, doi:10.1093/treephys/tpr143 (2012).

22 Körner, C. Carbon limitation in trees. *J Ecol* 91, 4-17, doi:DOI 10.1046/j.1365-2745.2003.00742.x (2003).

23 Mencuccini, M. *et al.* Size-mediated ageing reduces vigour in trees. *Ecol Lett* 8, 1183-1190, doi:DOI 10.1111/j.1461-0248.2005.00819.x (2005).

24 Burkhardt, J., Basi, S., Pariyar, S. & Hunsche, M. Stomatal penetration by aqueous solutions - an update involving leaf surface particles. *New Phytol* 196, 774-787, doi:DOI 10.1111/j.1469-8137.2012.04307.x (2012).

25 Yates, D. J. & Hutley, L. B. Foliar uptake of water by wet leaves of Sloanea-Woollsii, an australian subtropical rain-forest tree. *Aust J Bot* 43, 157-167, doi:Doi 10.1071/Bt9950157 (1995).

26 Eller, C. B., Lima, A. L. & Oliveira, R. S. Foliar uptake of fog water and transport belowground alleviates drought effects in the cloud forest tree species, Drimys brasiliensis (Winteraceae). *New Phytol* 199, 151-162, doi:Doi 10.1111/Nph.12248 (2013).

262 27 Fatichi, S., Leuzinger, S. & Korner, C. Moving beyond photosynthesis: from carbon
263 source to sink-driven vegetation modeling. *New Phytol* 201, 1086-1095, doi:Doi
264 10.1111/Nph.12614 (2014).
265 28 Leuzinger, S. *et al.* Do global change experiments overestimate impacts on terrestrial
266 ecosystems? *Trends Ecol Evol* 26, 236-241, doi:DOI 10.1016/j.tree.2011.02.011
267 (2011).

268

269

270

Figure Legends

Fig. 1| Changes in biomass and mortality rates. a. Biomass on the control and TFE plot from 2002-2014 (Mg C ha^{-1} yr^{-1}). Error bars show the s.e.m. calculated from 12 estimates of biomass, accounting for uncertainty in wood density and allometric equations (see Methods). b. Mortality rate (% stems $year^{-1}$) calculated separately for trees of 10-20 cm dbh, 20-40 cm dbh and >40 cm dbh on the control (black) and TFE (grey). The genus at date of death for each tree used in the mortality rate calculations is shown in Extended data Table 2.

Fig. 2| Tree growth of living and dead trees. a. Average annual stem increment in the four years prior to death for all trees which died on the control (n=35) and TFE (n=60) from 2005 onwards. Growth rates are normalised by the growth in year 0, the year in which the tree died. b-d. Stem increment for small (a. 10-20 cm dbh), medium (b. 20-40 cm dbh) and large (c. >40 cm dbh) trees on the control and TFE plot from 2005 to 2014. Values for b-d are normalised by the maximum increment on the control plot. Error bars show the s.e.m.

Fig. 3| Leaf, branch and stem NSC concentrations. Percentage values for soluble sugars (a.) and starch (b.) in dried biomass of leaves, branches and stems on the control and TFE for late dry season (November 2013), mid wet season (March 2014) and in the wet-to-dry transition (June 2014) for trees on the control (n=20) and TFE (n=21). Error bars show s.e.m. and * indicates a significant difference at $P < 0.05$ using the Wilcoxon test. June 2014 has significantly elevated sugar values on the TFE plot, however the absolute values for sugar concentration are very low, and the absolute differences are very small.

Figure 4| Xylem vulnerability to embolism and predicted loss of xylem hydraulic conductivity as a function of tree diameter (dbh). A general linear model was employed to test for the effects of genus and tree dbh on the estimates of xylem P_{50} obtained for each species (n=37 trees in total). The dashed lines give the predicted regressions for each of the

six genera, whereas the bold black line gives the overall mean regression line across all species (The adjusted R^2 in the figure refers to the overall model, while the P value refers to the significance of tree dbh). The insert shows the changes in predicted losses of hydraulic conductivity (PLC) as a function of tree size. In the main graph, each genus is represented with a different symbol and/or colour, as detailed in the legend. In the inset, the bold lines represent the average prediction for the most vulnerable genus (red: *Pouteria*) and for the most resistant one (blue: *Licania*) to drought induced embolism, with the shaded areas (pink, light blue) giving the respective 95% confidence intervals.

Extended data Figure 1| Leaf area index change: leaf area index (LAI; m^2 leaf area m^{-2} ground area) for the period of 2001-2014 on the control (black, solid) and TFE (grey, dashed) plots. Error bars show the s.e.m. associated with LAI calculation (see Methods).

Extended Data Fig. 2| Seasonal soil water potential: average soil water potential (- MPa) in the control and TFE during dry season (July-December) and wet season (January-June), calculated form monthly average volumetric soil moisture content data, collected from 2008-2014, using sensors installed 0, 0.5, 1, 2.5 and 4 m below the surface and the necessary van Genuchten parameters previously calculated from soil hydraulics measurements at this site (see Methods). They are averaged from hourly data collected from 2008-2011 and error bars show s.e.m.

Extended data Figure 3| Leaf herbivory comparison: average percentage loss of leaf area from herbivore attack calculated from 9770 leaves collected in litter-traps on the control and TFE plot from 2010-2014. Error bars show s.e.m. A separate analysis of herbivore attack on 13,694 top-canopy living leaves from branches of the 41 trees used for the P_{50} analysis

support these results, also showing no significant differences in percentage herbivory between the control and the TFE (data not shown).

Extended Data Figure 4| Diurnal patterns of Ψ_l: diurnal Ψ_l measured every 2 hours from 6.00 until 18.00 in dry season on trees accessible from the walk up tower. Each box shows the diurnal Ψ_l against diurnal air vapour pressure deficit (VPD) from one of seven trees accessible on the control (C), or one of four trees accessible on the TFE. Note a majority of trees demonstrate some a negative relationship with VPD. Combined separately for each plot, a significant negative linear relationship is observed between Ψ_l and VPD on the control (R^2=0.18, P=0.002) and even more strongly on the TFE (R^2=0.33, P=0.001).

Methods

Site: The through-fall exclusion (TFE) experiment is located in the Caxiuanã National Forest Reserve in the eastern Amazon (1°43'S, 51°27W), ~400 km west of the nearest city, Belém, State of Pará, Brazil. The experiment is located in *terra firme* forest, on yellow oxisol soils which are 75-83 % sand, 12-19 % clay and 6-10 % silt[29]. The site is 15 m above sea level, has a mean annual rainfall between 2000-2500 mm and a pronounced dry season between June and November[2].

The experimental site has two 1 ha plots: the TFE, over which plastic panels and gutters have been placed at a height of 1-2 m, and which exclude 50% of the incident rainfall; and a corresponding control plot, <50 m from the TFE, on which there has been no manipulation of incident rainfall. The TFE was trenched to between 1-2 m to remove the effect of through-flow of soil water; and to control for any temporary damage to roots from the trenching, the control plot was also trenched to the same depth. The TFE treatment has been installed and running continuously since January 2002 to the present, except for a 1 week period in November 2002 (full removal), a month period during the dry season in November 2014 (sequential removal of all panel) and during 2004 (30% removal).

Soil Moisture Data: In both the control and TFE plots there are soil access pits in which volumetric soil water content sensors (CS616, Campbell Scientific, Logan, USA) located at depths of 0, 0.5, 1, 2.5 and 4 m, monitor soil moisture every hour (*cf*. Fisher et al.[30], for full methodology). New data presented here are from March 2008 - December 2014, averaged into monthly values. Due to equipment failure, some soil moisture data are missing for August and December 2013, for 2008 and 2010 on the control plot, and for November and December 2013 on the TFE plot. Volumetric soil water content was converted in to soil water

potential (Ψ_s) using the necessary van Genuchten parameters previously calculated by Fisher et al.[31] based on soil hydraulics measurements at this site.

Biomass data: Trees ≥10 cm diameter at breast height (dbh) on both the control and the TFE plots were tagged and identified to species level in September 2000. Diameters were measured on these trees at 1.3 m, unless buttress roots were present, in which case the measurement was made above the buttressing. Individuals on the plots were re-censused at varying intervals from January 2001, until November 2014. During each census the trees were also assessed to be either dead or alive. A tree was considered dead if leaflessness was accompanied by a persistent zero or negative stem increment, and/or the tree had snapped or fallen to the ground. Recruitment of new trees into the ≥10 cm dbh size class was enumerated in 2005, 2009 and 2014.

Trees in the 10 x 10 m subplots adjacent to the trenches were excluded from our biomass and growth rate analysis to eliminate possible effects of changes in mortality resulting from root damage[2]. Consequently, 369 trees on the control and 358 trees on the TFE, each in 0.64 ha were analysed and the biomass scaled to 1 ha. Following da Costa et al. (2010)[6] trees were grouped into small (10-20 cm dbh) and medium (20-40 cm dbh) and large (>40 cm dbh) size classes.

Biomass was calculated using the Chave et al.[32] equation which uses diameter, wood density and environmental predictors. A mean and standard deviation of wood density for each tree was calculated from data in the global wood density database[33,34] and from Patiño et al.[35]. Multiple estimates of wood density at the species, genus and family level were used to calculate standard deviations on our wood density estimates. Of all the trees on both plots, 68 % had values for wood density at species level, 18 % at genus level and 3 % at family level; 11 % of trees were not identified and were given a plot level average wood density with an

associated standard deviation. A standard error on our biomass estimations was calculated, which accounted for the error associated with wood density estimation and variations in commonly used allometric equations. Twelve calculations were used to calculate the error on our biomass values; these 12 biomass estimates were from combinations of four biomass equations: Chave et al.[32] and Chave et al.[36] both with and without height and three wood density estimates: mean wood density and mean wood density ± one standard deviation. The allometric equations selected represent one of the most commonly used biomass equations for Amazonia[36] (with and without height as a predictor variable) and the most recent and most comprehensive biomass equations for our study area[32] (with and without height as a predictor variable). Measurements of height were not available and were calculated from an equation developed specifically for the region of the Amazon in which our plots are located[37]. Mortality rate was calculated according to da Costa et al. (2010)[6] and separately for trees of 10-20 cm dbh, 20-40 cm dbh and >40 cm dbh on the TFE and control plot.

Seasonal growth data: Dendrometers were installed at just above or below the point of dbh measurement on all trees ≥10 cm dbh[38]. Circumference measurements from the dendrometer bands were made monthly to tri-monthly from January 2005 to November 2014, with the exception of a six month gap from July 2007 and January 2013. Seasonal shrinkage was calculated by taking the average growth rate of 19 trees on the control and TFE plots which experienced no overall growth, but demonstrated a seasonal pattern of shrinkage and expansion. Tropical trees can experience net diameter shrinkage in the dry season, due to a lack of growth, accompanied by reduced water content of stem tissues, with subsequent swelling when tissues are rehydrated in the wet season[39]. An average pattern of shrinkage and expansion was therefore subtracted from all trees to ensure that dry season growth was not under-estimated and wet season growth over-estimated. Dendrometer increments were filtered to remove the growth spikes from measurement errors following Rowland et al.

(2014)[39]. Subsequent to this procedure, gap-filling was done using linear interpolation[39]; on the control and TFE plot 16 % and 17 % of the data were gap-filled respectively. Growth rates per day calculated from the dendrometer measurements were averaged into three monthly periods to give continuous tri-monthly growth rates from 2005-2014. When trees in the 10 x 10 m subplots adjacent to the trenches, and trees with poor quality dendrometer measurements throughout the 10 year study period for growth were excluded, 316 and 310 trees on the control and TFE plot remained, respectively. All growth and mortality analyses were done using the R statistical package (version 3.1.2). Tests for significance were performed using Wilcoxon signed-rank test.

Non Structural Carbohydrate (NSC) analysis. Using samples cut by a tree climber from fully sunlit branches, three leaves and a branch sample of ~ 8-10 mm diameter were taken from 20 trees on the control plot and 21 trees on the TFE plot in November 2013, March 2014 and June 2015. The numbers and species of the trees selected for analysis are shown in Extended Data Table 1. The selected trees were all >10 cm dbh and represented the most common genera existing on both plots[2]; samples were not taken from the external 10 x 10 m subplots to avoid any impacts of trenching. Samples of tree stem tissue from the same trees were taken with a 5 mm increment borer at breast height once in November 2013; this sampling was not repeated to avoid excessive damage incurred by repeated boring. We followed the enzymatic method proposed by Sevanto et al. (2014)[40] to analyze the NSC content. Here, NSC is defined as free, low molecular weight sugars (glucose, fructose and sucrose) and starch. Immediately after collection, samples were microwaved to stop enzymatic activity. After that, samples were oven-dried at 70°C for 24–48 h and ground to fine powder. We prepared approximately 12 mg of plant material with 1.6 mL of distilled water for the analysis. We used amyloglucosidase from *Aspergillus niger* (Sigma-Aldrich) to digest total NSC to glucose, and invertase, glucose hexokinase kits (GHK) and phosphorus glucose (Sigma-

427 Aldrich) to quantify the low molecular weight sugars. The concentration of free glucose was
428 determined photometrically in a 96-well microplate spectrophotometer (BioTek, Epoch).
429 NSC values are expressed as percent of dry matter. For further method details, see Sevanto et
430 al. (2014)[40].

431 *Xylem vulnerability to cavitation (Percentage Loss of Conductivity; PLC) and leaf water*
432 *potential measurements*. Samples were cut from fully sunlit branches following the same
433 protocol as above for NSC during late dry season (November 2013), and using the same
434 sample trees as used for the NSC analysis (Extended Data Table 1), with the exception of
435 branches of the genus *Manilkara*. To maintain a balance of number of genera and trees
436 sampled, four additional trees were therefore sampled from the genus *Inga* in the TFE and
437 control plots for both sets of analyses. One to three 1.0-1.5 m long branches per tree were cut
438 and left to rehydrate overnight under a black plastic bag in a bucket of water. Maximum
439 vessel length was determined for one branch out of a set of 5-6 branches for each species by
440 injecting low pressure air at the branch base under water and progressively re-cutting the
441 stem until bubbles emerged (maximum conduit length varied between 25 and 50 cm across
442 samples)[41]. Axial slits were made in the branch segments selected for PLC analysis to
443 increase the efficacy of the air injection. These partially debarked segments were mounted on
444 a 4.6 cm long air injection apparatus. Water, filtered to 0.2 μ, flowed gravimetrically through
445 the sample. After 10 minutes of equilibration at low pressure (10 kPa), the sample was
446 pressurised for 20 min. The pressure was increased in steps of 0.3 to 0.5 MPa, with each step
447 followed by 10 min relaxation and flow measured at a constant background 100 kPa air
448 pressure, until a residual flow lower than 5 % of the initial flow was found. Five to 10
449 measurements of water flux were taken at the distal end. The interval for each conductivity
450 measurement ranged from 2 to 10 minutes depending on stem length, conductivity and

pressure head employed (normally 3 kPa). Segment lengths, cross-sectional diameters and leaf areas of the leaves subtended by the measured segment were determined.

We employed a two-parameter Weibull function to model the changes in percent loss of xylem hydraulic conductivity as a function of xylem pressure[42]. The two parameters represented P_{50} and slope of the conductivity-pressure curve. We estimated P_{50} and slope for all trees using tree as a random factor in a mixed-model analysis (nlme library[43]) in R (Version 3.02, R Core Team). We let P_{50} vary for each tree while keeping slope constant across trees to achieve convergence. We then employed these conditional estimates of P_{50} in a general linear model to test for the effects of plot, genus and dbh (Extended Data Table 3a).

We then confirmed the above results by running a second mixed-effect model, in which we accounted for random tree-by-tree variation and variance driven by phylogeny, by nesting individual trees within genera as the random component of the model and incorporating plot and dbh as fixed effects (Extended Data Table 3b). We tested whether tree diameter affected P_{50} by comparing the performance of the full model with the same model without the effect of dbh on P_{50} using a likelihood ratio test, and by conducting simultaneous hypothesis tests at the 95% significance level (library multcomp in R). For both analyses, distributional assumptions were tested by looking at plots of residuals for fixed and, if the case, random effects.

Leaf water potential Ψ_l was measured during two campaigns (one during the dry and one during the wet season, i.e., October 2013 and May 2014, respectively). Two to four leaves were measured for each branch of each tree, following the same sampling protocol above for NSC and hydraulic measurements. During each campaign, Ψ_l measurements were conducted at pre-dawn (prior to 07.00 hrs) and at midday (between 11.30 hrs and 1300 hr). Midday Ψ_l measurements of both campaigns were used in conjunction with the P_{50} and slope values

475 determined for each genus to estimate percent loss of hydraulic conductivity (PLC), assuming
476 xylem water potential to be equal to measured leaf water potential[20]. We acknowledge that
477 this may overestimate PLC; however in counterpoint, only one seasonal campaign could be
478 conducted and so the minimum of leaf Ψ_l for that year was thus likely to have been
479 underestimated because fuller sampling through the dry season was impractical. In addition,
480 earlier (2003) studies in the same experiment[44] reported minimum values of stem xylem
481 water potentials of around -1.6 MPa, across control and TFE plots, suggesting that xylem
482 values substantially more negative than those assumed here can be experienced.

483 *Herbivory:* All leaf material from 25 x 1 m^2 litter-traps on the control and TFE was collected
484 13 times from 2010-2014 at 3-6 month intervals, with one eight month interval in 2011. Each
485 collection of leaf material represented two weeks of litter-fall in the forest. The 9770 leaves
486 collected from all 25 per plot litter-traps over the study period were scanned and the images
487 were analysed according to Metcalfe et al.[45] to calculate the percent leaf area lost to herbivore
488 attack on the control and TFE.

489 *LAI measurements*: LAI values from 2001 to 2007 are taken from Figure 1f in Metcalfe et al.
490 (2010)[38]. For 2009-2014 LAI was measured at the same 25 permanent points[38] on a grid
491 throughout the control and TFE plot. Measurements were made using hemispherical photos
492 taken every 3-6 months from 2009-2014. Photos were taken before sunrise (~6.00 am) from a
493 height of 1.5 m on the control plot and 2 m (above the TFE structure) on the TFE plot. The 25
494 photos per plot were analysed together using the CAN_EYE software (INRA, Avignon,
495 France). Standard errors were calculated using three different estimates of LAI given by the
496 CAN_EYE software.

Extra References for Methods

29 Ruivo M & E., C. in *Ecosystems and sustainable development.* (ed E. Tiezzi, Brebbia, C. A., Uso, J. L., (eds)) 1113–1121 (WIT Press, 2003).

30 Fisher, R. A. *et al.* The response of an Eastern Amazonian rain forest to drought stress: results and modelling analyses from a throughfall exclusion experiment. *Global Change Biol* 13, 2361-2378, doi:DOI 10.1111/j.1365-2486.2007.01417.x (2007).

31 Fisher, R. A., Williams, M., Ruivo, M. D., de Costa, A. L. & Meira, P. Evaluating climatic and soil water controls on evapotranspiration at two Amazonian rainforest sites. Agr Forest Meteorol 148, 850-861, doi:DOI 10.1016/j.agrformet.2007.12.001 (2008).

32 Chave, J. *et al.* Improved allometric models to estimate the aboveground biomass of tropical trees. *Global Change Biol* 20, 3177-3190, doi:Doi 10.1111/Gcb.12629 (2014).

33 Chave, J. *et al.* Towards a worldwide wood economics spectrum. *Ecol Lett* 12, 351-366, doi:DOI 10.1111/j.1461-0248.2009.01285.x (2009).

34 Zanne, A. E. *et al*. Data from: Towards a worldwide wood economics spectrum. Dryad Digital Repository. http://dx.doi.org/10.5061/dryad.234. (2009).

35 Patiño, S. *et al.* Branch xylem density variations across the Amazon Basin. *Biogeosciences* 6, 545-568, doi:DOI 10.5194/bg-6-545-2009 (2009).

36 Chave, J. *et al.* Tree allometry and improved estimation of carbon stocks and balance in tropical forests. *Oecologia* 145, 87-99, doi:DOI 10.1007/s00442-005-0100-x (2005).

37 Feldpausch, T. R. *et al.* Tree height integrated into pantropical forest biomass estimates. *Biogeosciences* 9, 3381-3403, doi:DOI 10.5194/bg-9-3381-2012 (2012).

38 Metcalfe, D. B. *et al.* Shifts in plant respiration and carbon use efficiency at a large-scale drought experiment in the eastern Amazon. *New Phytol* 187, 608-621, doi:DOI 10.1111/j.1469-8137.2010.03319.x (2010).

39 Rowland, L. *et al.* The sensitivity of wood production to seasonal and interannual variations in climate in a lowland Amazonian rainforest. *Oecologia* 174, 295-306, doi:DOI 10.1007/s00442-013-2766-9 (2014).

40 Sevanto, S., McDowell, N. G., Dickman, L. T., Pangle, R. & Pockman, W. T. How do trees die? A test of the hydraulic failure and carbon starvation hypotheses. *Plant Cell Environ* 37, 153-161, doi:Doi 10.1111/Pce.12141 (2014).

41 Ennajeh, M., Simoes, F., Khemira, H. & Cochard, H. How reliable is the double-ended pressure sleeve technique for assessing xylem vulnerability to cavitation in woody angiosperms? *Physiol Plantarum* 142, 205-210, doi:DOI 10.1111/j.1399-3054.2011.01470.x (2011).

42 Neufeld, H.S., Grantz, D.A., Meinzer, F.C., Goldstein, G., Crisosto, G.M. & Crisosto. C. Genotypic variability in vulnerability of leaf xylem to cavitation in water-stressed and well-irrigated sugarcane. Plant Physiol. 100:1020—1028 (1992).

43 Pinheiro, J. C. & Bates, D. M. *Mixed-Effects Models in S and S-PLUS*. (Springer, 2000).

44 Fisher, R. A., Williams, M., Do Vale, R. L., Da Costa, A. L. & Meir, P. Evidence from Amazonian forests is consistent with isohydric control of leaf water potential. *Plant Cell Environ* 29, 151-165, doi:DOI 10.1111/j.1365-3040.2005.01407.x (2006).

45 Metcalfe, D. B. *et al.* Herbivory makes major contributions to ecosystem carbon and nutrient cycling in tropical forests. *Ecol Lett* 17, 324-332, doi:Doi 10.1111/Ele.12233 (2014).

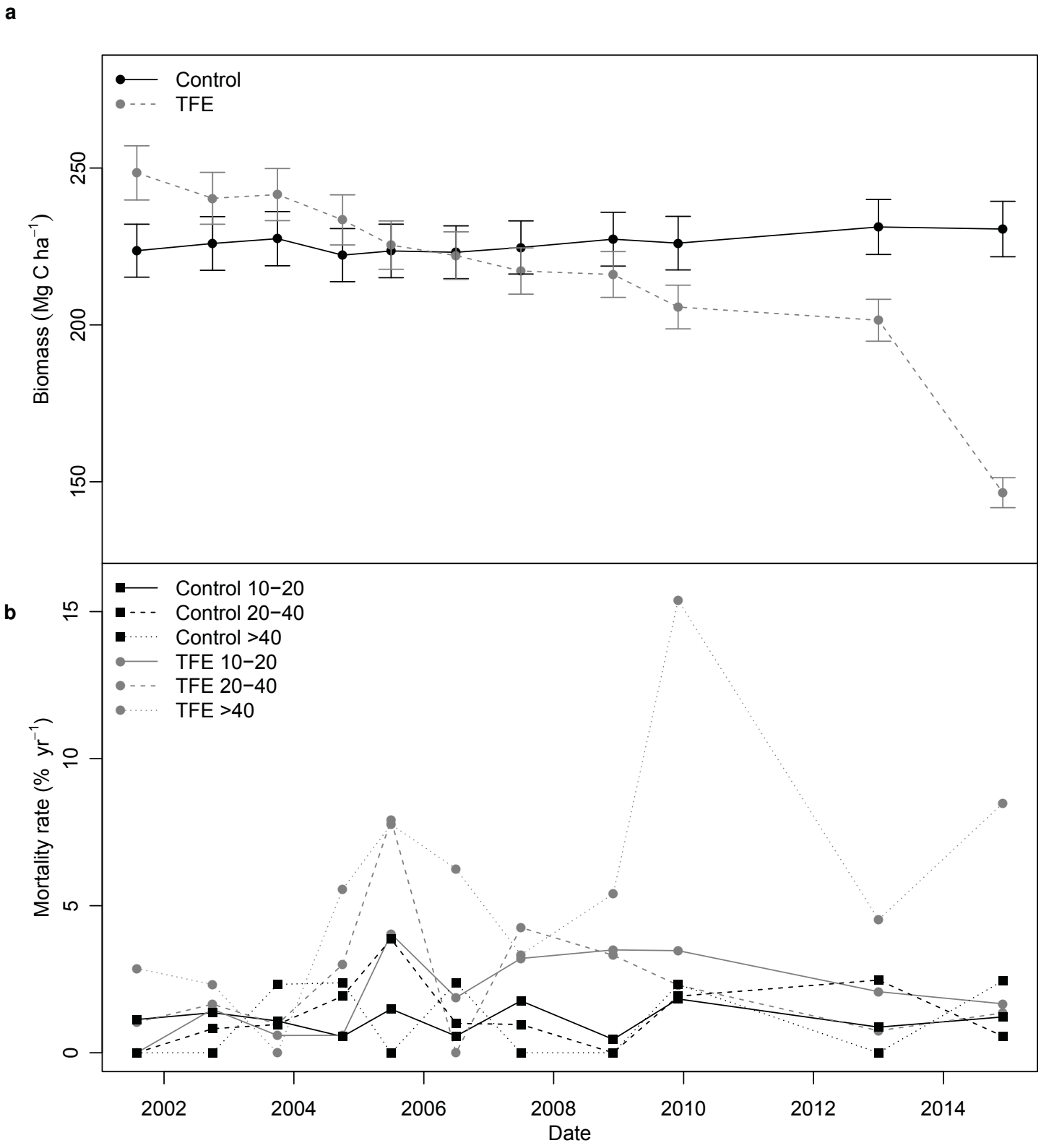
a
Control
TFE
Biomass (Mg C ha^{-1})
150
200
250
b
Control 10−20
Control 20−40
Control >40
TFE 10−20
TFE 20−40
TFE >40
Mortality rate (% yr^{-1})
0
5
10
15
2002
2004
2006
2008
2010
2012
2014
Date

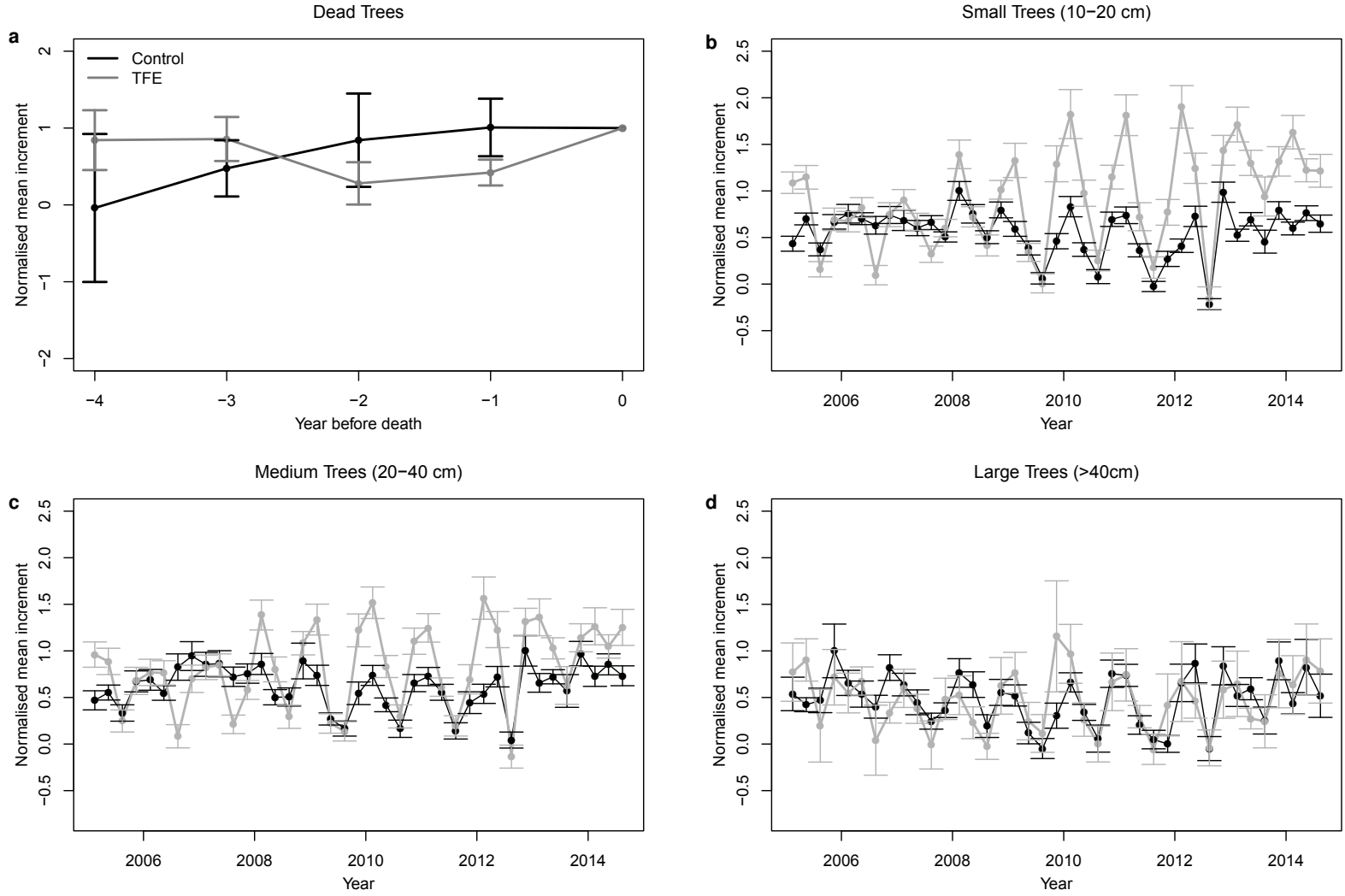
Dead Trees
a
Control
TFE
Normalised mean increment
Year before death
−4
−3
−2
−1
0
Small Trees (10−20 cm)
b
Year
2006
2008
2010
2012
2014
Medium Trees (20−40 cm)
c
Large Trees (>40cm)
d

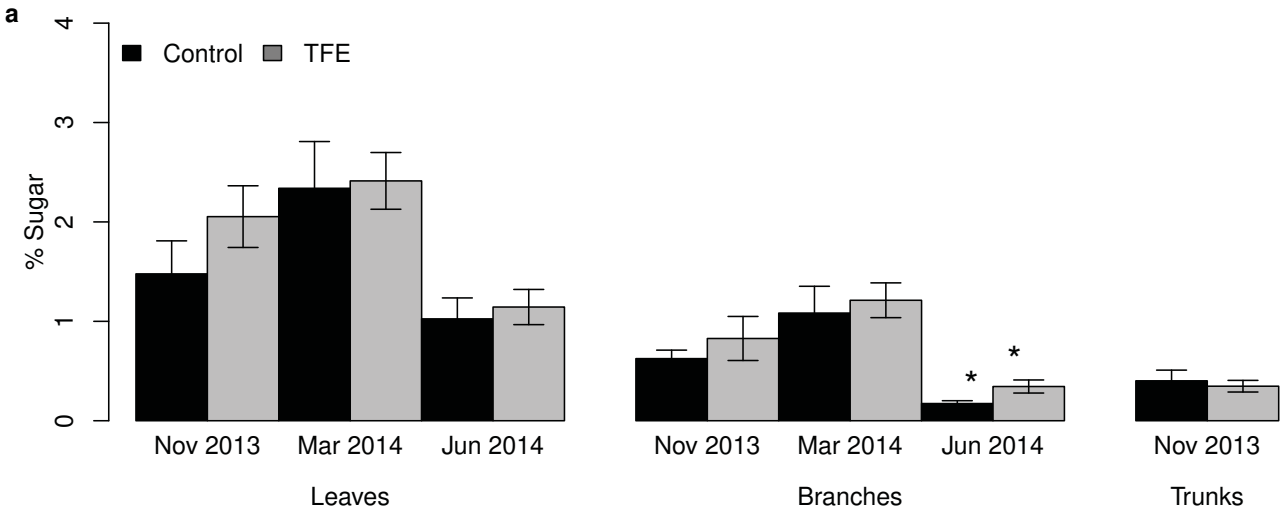
a
Control
TFE
% Sugar
0
1
2
3
4
*
*
Nov 2013
Mar 2014
Jun 2014
Leaves
Nov 2013
Mar 2014
Jun 2014
Branches
Nov 2013
Trunks

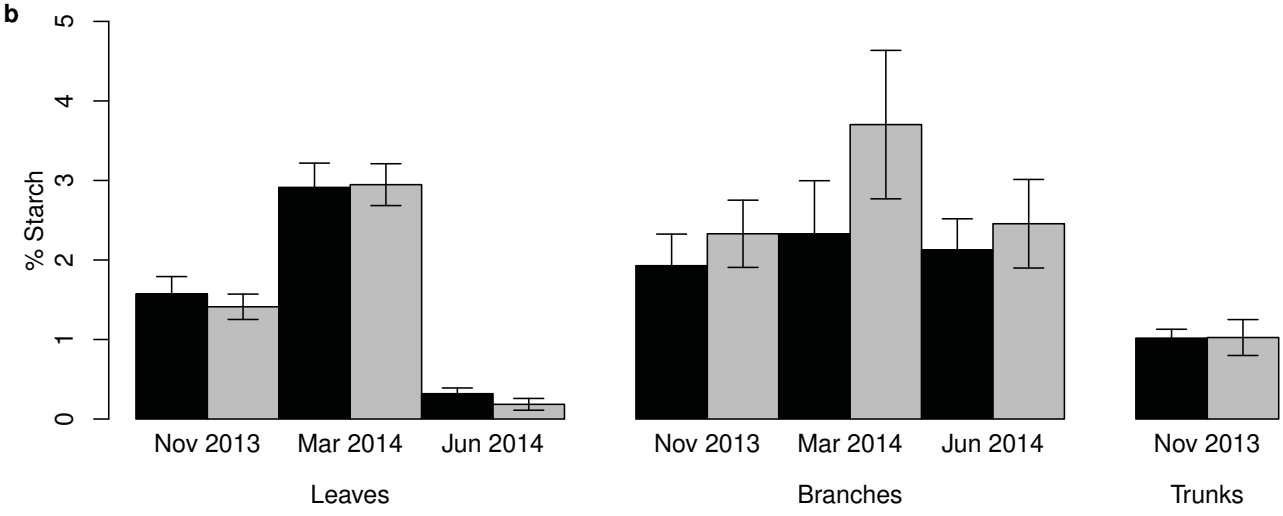
b
% Starch
0
1
2
3
4
5
Nov 2013
Mar 2014
Jun 2014
Leaves
Nov 2013
Mar 2014
Jun 2014
Branches
Nov 2013
Trunks

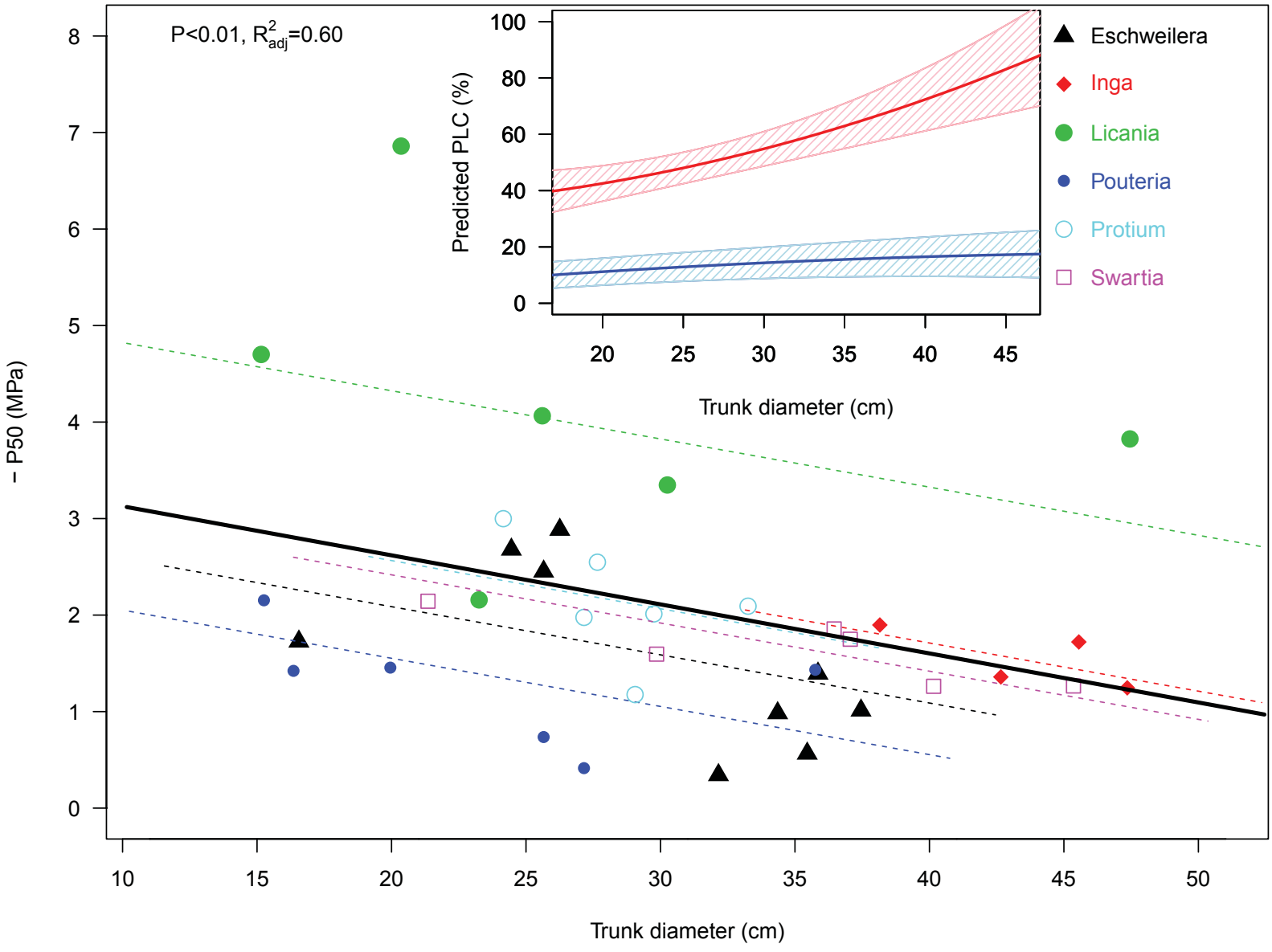
P<0.01, R^2_{adj}=0.60
– P50 (MPa)
Trunk diameter (cm)
Predicted PLC (%)
Trunk diameter (cm)
Eschweilera
Inga
Licania
Pouteria
Protium
Swartia